THE JOURNAL OF COMPARATIVE NEUROLOGY 387:358–370 (1997)

Optically Imaged Maps of Orientation Preference in Primary Visual Cortex of Cats and Ferrets

S. CHENCHAL RAO, LOUIS J. TOTH, AND MRIGANKA SUR*
Department of Brain and Cognitive Sciences, Massachusetts Institute of Technology, Cambridge, Massachusetts 02139

ABSTRACT

Feature maps in the cerebral cortex constitute orderly representations of response features created within the cortex; an example is the mapping of orientation-selective neurons in visual cortex. We have compared the properties of orientation maps in area 17 of cats and ferrets, obtained by optical imaging of intrinsic signals. Orientation maps in both species contain a quasi-periodic distribution of iso-orientation domains that are organized into a lattice of pinwheels. However, the spatial density of orientation domains and of pinwheels in ferret area 17 is nearly twice that in cat area 17. The ferret map also contains more discontinuities, or fractures, where orientation changes abruptly. The size of orientation domains scales with interdomain spacing, so that the ratio of the two is approximately the same in both species. Consistent with this finding, the orientation tuning width of individual pixels is similar in the two. The magnitude of orientation preference, however, is much lower in ferret compared to cat. The greater incidence of fractures in ferret appears to be due to proportionately greater overlap between domains of different orientations, particularly along fracture lines that link pinwheel centers. We hypothesize that a key determinant of orientation maps, the relationship between orientation domain size and spacing, expresses an anatomical link between sizes of thalamocortical arbors and horizontal intracortical connections in area 17. J. Comp. Neurol. 387:358–370, 1997. © 1997 Wiley-Liss, Inc.

Indexing terms: area 17; intrinsic signals; tuning; orientation fracture; orientation domains

A ubiquitous theme in cortical organization is the orderly mapping of neuronal responses within a cortical area. A fundamental mapping in sensory cortex is the topographic representation of a sensory epithelium; examples of such maps are the retinotopic map of visual space in primary visual cortex or the somatotopic map of the body surface in primary somatosensory cortex (Kaas, 1988). The rules of topographic maps are well understood: The maps in primary visual or somatosensory cortex, for example, arise by the orderly projection of adjacent sets of thalamic fibers relayed to cortex, with different regions of the map containing variable proportions of inputs that lead to variations in magnification and concomitant changes in receptive field size (Hubel and Wiesel, 1974; Sur et al., 1980; see also Merzenich et al., 1983).

A different kind of map relates to the representation of response features created within the cortex, often as an emergent property of cortical circuitry. An example of such a map is the organization of orientation-selective cells in visual cortex. Although basic features of the mapping of orientation selectivity has been described with both single unit recording (Hubel and Wiesel, 1974) and optical imaging (Bonhoeffer and Grinvald, 1993), a systematic comparison of the basic properties of orientation maps in different species has yet to be done. We have analyzed orientation maps obtained by optical imaging of intrinsic signals in area 17 of two closely related species, cats and ferrets. In particular, we have compared the two fundamental units of organization of the orientation system, viz. orientation domain size and the interdomain spacing, along with the strength of the response feature itself, viz. the magnitude of orientation preference. We reasoned that such a comparison would also provide testable hypotheses regarding possible determinants of a feature map such as that for orientation.

Grant sponsor: NIH; Grant number: EY07023.

Dr. S.C. Rao's present address is: Vanderbilt Vision Research Center, Dept. of Psychology, Wilson Hall, Vanderbilt University, Nashville, TN 37240.

Dr. L.J. Toth's present address is: Department of Neurobiology, Harvard Medical School, 220 Longwood Ave., Boston, MA 02115.

*Correspondence to: Mriganka Sur, Department of Brain and Cognitive Sciences, M.I.T., E25-235, Cambridge, MA 02139.
E-mail: msur@wccf.mit.edu

Received 8 November 1996; Revised 15 April 1997; Accepted 21 May 1997

© 1997 WILEY-LISS, INC.

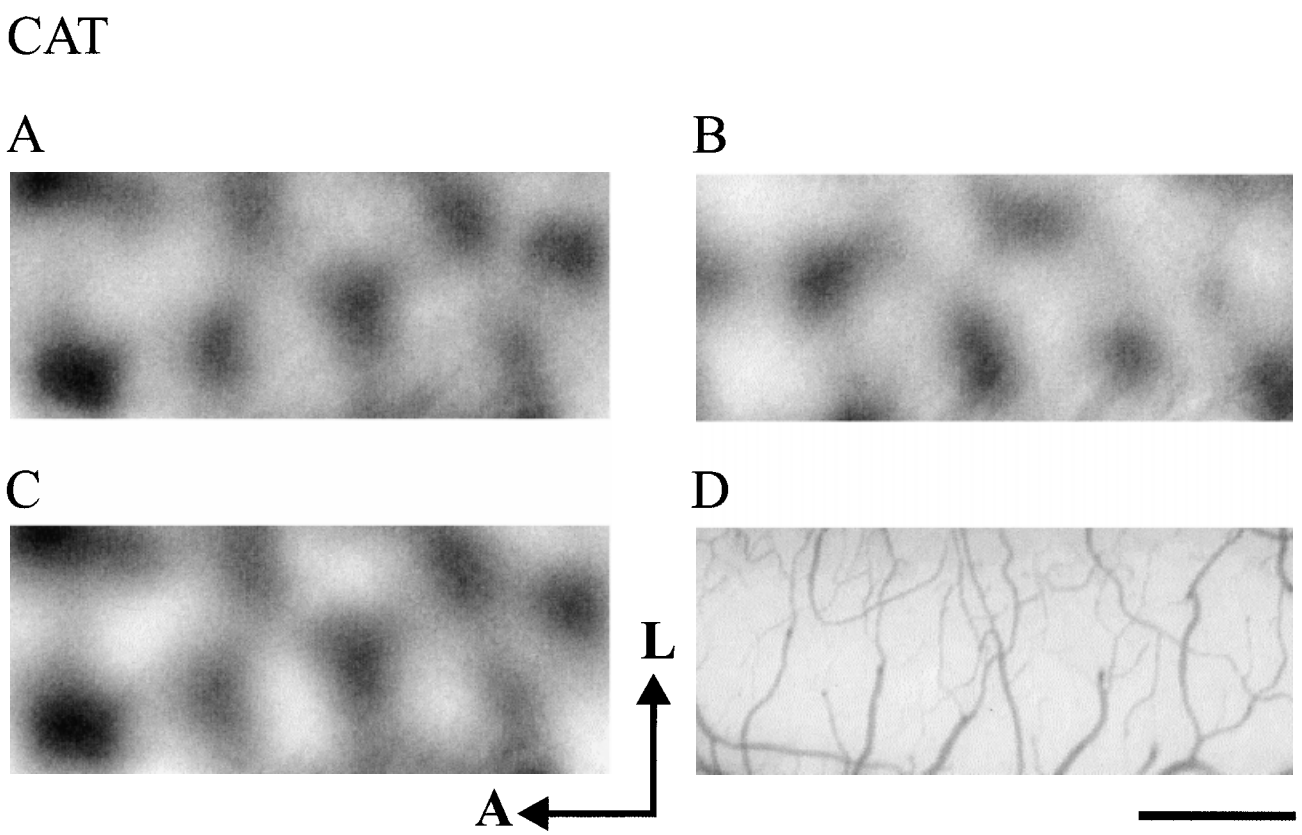

Fig. 1. Orientation specific intrinsic signals from cat area 17. **A:** Single-orientation map showing iso-orientation domains of cortical activity (dark areas represent higher activity) in response to moving gratings oriented at 22.5° (images for gratings moving in opposite directions were summed). **B:** Single-orientation map as in A, but in response to gratings of the orthogonal orientation, 112.5°. Note that these orthogonal grating stimuli activate complementary spatial locations in the cortex. **C:** Contrast enhancement achieved by dividing the single-orientation map in A by that in B. **D:** Pattern of cortical vasculature in the imaged region. A, anterior; L, lateral. Scale bar = 1 mm.

MATERIALS AND METHODS

Surgery and recording chamber placement

Experiments were done under protocols approved by MIT's Animal Care and Use Committee. Female cats aged 10 weeks to adult and adult female ferrets were initially anesthetized with a mixture of ketamine (cat 15 mg/kg; ferret 25 mg/kg, i.m.) and xylazine (1.5 mg/kg, i.m.). Subsequently, anesthesia was maintained by continuous infusion of sodium pentobarbital (1.5–2 mg/kg/hr, i.v.) added to a 50/50 mixture of 5% dextrose and lactated Ringer's solution for fluid maintenance. A tracheotomy was performed to faciliate artificial ventilation. The animal's heart rate and electroencephalogram (EEG) were continuously monitored to ensure adequate levels of anesthesia. Expired CO_2 was maintained at 4% by adjusting the stroke volume and the rate of the respirator. The animal was placed on a heating blanket, and the rectal temperature was maintained at 38°C. In cats, a bilateral craniotomy and durotomy were performed, extending from Horsley-Clark coordinates AP0 to roughly 7 mm posteriorly and from the midline to 4 mm laterally. In ferrets, the craniotomy extended from the posterior cortical pole, initially located by using the tentorial ridge as a guide, to 4 mm anteriorly and from the midline to 7 mm laterally. After completion of surgery, paralysis was initiated with gallamine triethiodide (10 mg/kg/hr) to prevent eye movements. A stainless steel chamber (20 mm diameter) was cemented to the skull with dental acrylic, and the inner margin was sealed with wax. In order to minimize cortical pulsations due to respiration and heartbeat, the chamber was filled with silicone oil and sealed with a transparent quartz window.

Optical recording

The cortical surface was illuminated with a bifurcated fiber-optic light guide attached to a 100-W tungsten-halogen lamp source powered by a regulated power supply. The light was passed through an infrared filter and filters of appropriate center wavelength and was adjusted for even illumination of the cortical surface at an intensity within the linear range of the camera's sensitivity. We used a slow-scan video camera (Bischke CCD-5024N, Japan, RS-170, 30 Hz) fitted with a macroscope (Ratzlaff and Grinvald, 1991), consisting of two back-to-back camera lenses (50 mm *f*1.2, toward camera and 55 mm *f*1.2, toward subject) that allowed both a high numerical-aperture and a shallow depth of field. The camera was focused on the cortical surface by emphasizing the vasculature using light of 540 nm. After the pattern of cortical vasculature was imaged, the camera was focused 300 mm below this plane to minimize blood-vessel artifacts. Light of 600 nm (10 nm bandpass) was used to image activity-dependent intrinsic oximetric signals. Data collection was under the

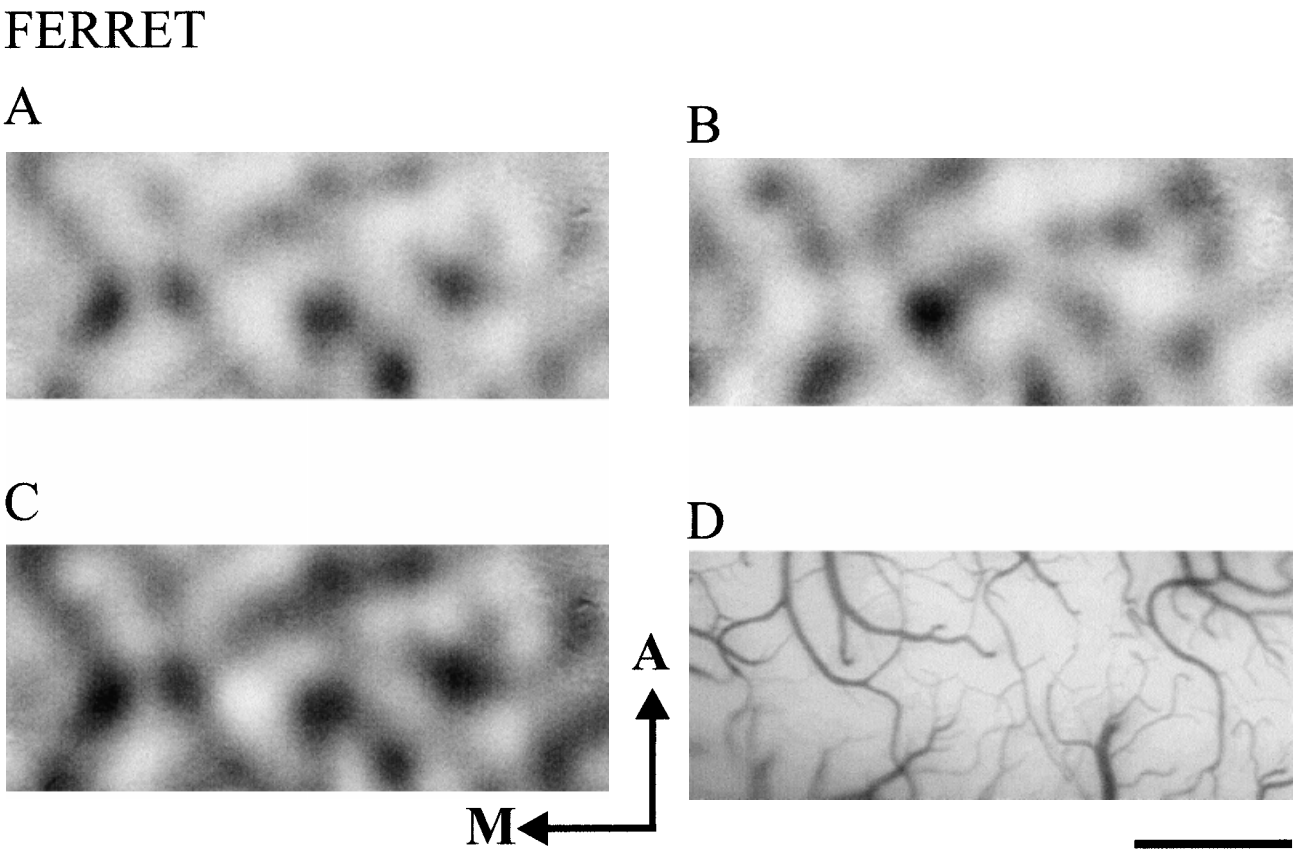

Fig. 2. Orientation specific intrinsic signals from ferret area 17. **A:** Single-orientation map imaged in response to moving gratings of 0° orientation. **B:** Single-orientation map in response to moving gratings of orthogonal orientation (90°). **C:** Differential image obtained by dividing map A by map B. **D:** Pattern of cortical vasculature in the imaged region. A, anterior; M, medial. Scale bar = 1 mm.

control of a hardware and software system (Imager 2001, Optical Imaging Inc., Durham, NC) which performed analog subtraction of a stored reference image (collected during presentation of a neutral gray screen) from the stimulus image (collected during presentation of an oriented grating), such that the image could be digitized in real time (Matrox image processor, Matrox Electronic Systems, Quebec, Canada, 8 bit, 15 MHz).

Visual stimulation

Eyes were fitted with appropriate contact lenses and focused on a monitor placed 30 cm in front of the animal. Eye position was checked by projecting the location of the optic disk onto a screen in front of the monitor with a reversing ophthalmoscope. Refraction was judged by slit retinoscopy and direct opthalmoscopy. The presence of a strongly reflective retinal epithelium in cats also allowed judgment of refraction by reverse opthalmoscopy (focusing the pattern of retinal vasculature onto the display screen directly). Only minimal correction was required in ferrets, because the smaller pupil diameter provides a naturally large depth of field. All visual stimuli, presented binocularly, were generated by a computer (486 PC) running STIM (K. Christian, Rockefeller University), using a Sgt. Pepper+ graphics board with 4 MB memory (Number Nine Corp., Lexington, MA) at a resolution of 640 × 480 pixels (60 Hz frame rate) on a Sony Trinitron 17-inch monitor. Individual frames of the stimuli were computed prior to the experiment and shown under the timing control of the data-collection computer. Moving full-field square-wave gratings (typical spatial frequency 0.375 cyc/deg) were shown as sets of 8 orientations (i.e., 22.5° apart). Grating orientations were randomly interleaved, and responses to opposite directions of motion were collected separately. Parameters of stimulus presentation and data collection were chosen to maximize the optical signal, as determined by our initial experiments and by previous reports of optical imaging in cat area 18 (Bonhoeffer and Grinvald, 1993). Each stimulus was shown in a stationary position for 5 seconds, and then drifted at a temporal frequency of 1.5 Hz for the duration of data collection.

Data analysis

The timing of data collection was chosen, based on pilot experiments, to bracket the time of maximum signal strength. Camera frames at 30 Hz, collected between 400 ms and 5,500 ms after the start of stimulus motion, were summed into 5–8 larger time blocks. Frames between approximately 1,300 ms and 4,600 ms after the start of stimulus motion were selected for further analysis. Two kinds of maps were derived from the raw data (Bonhoeffer and Grinvald, 1993). Single-orientation maps of responses to a grating at one orientation were obtained by dividing the summed activity in response to all presentations of a

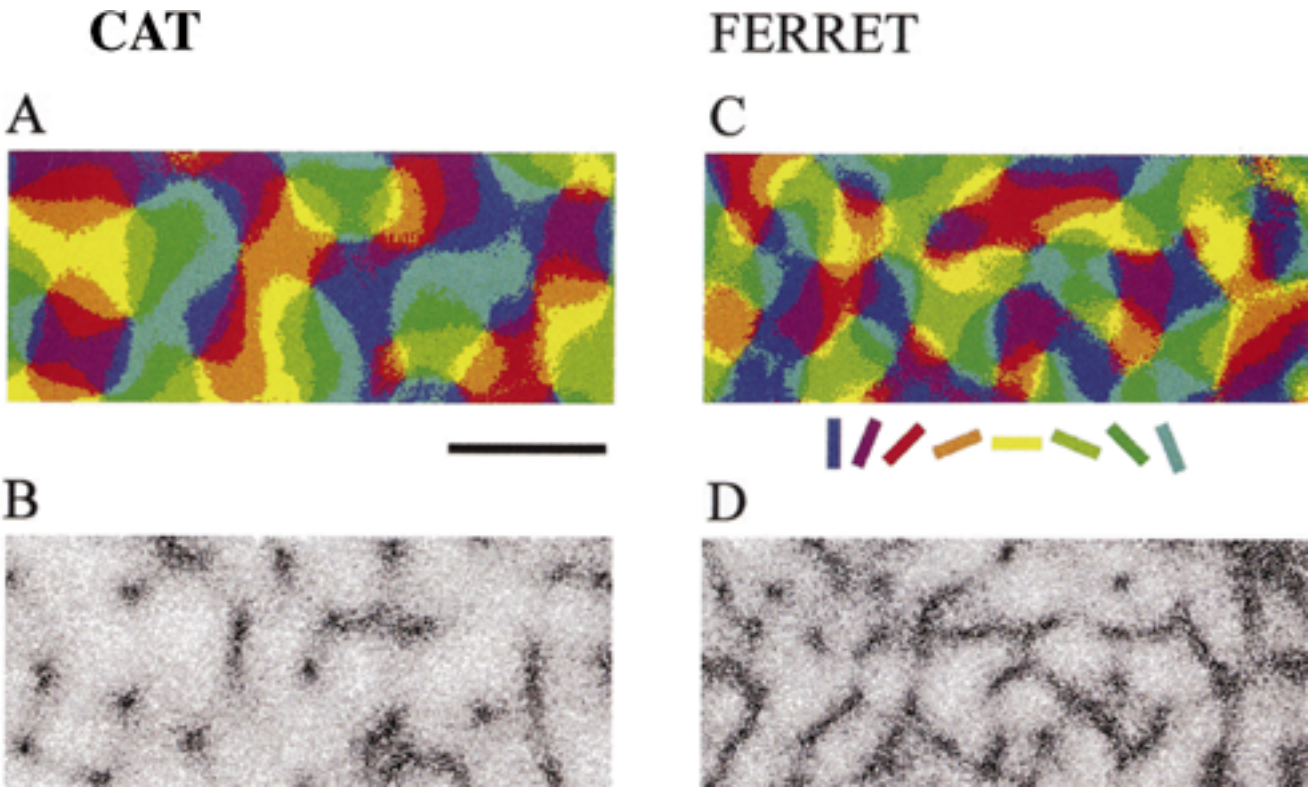

Fig. 3. Organization of orientation preference in cat and ferret area 17. **A:** Composite orientation preference map of cat area 17 obtained by vector averaging, pixel-by-pixel, the signal from eight single-orientation maps. The eight maps were obtained in response to moving gratings of orientations spaced 22.5° apart. **B:** Gradient map obtained from A showing the rate of change of orientation preference across the cortical surface. This map was obtained by applying a two-dimensional gradient operator to the orientation preference map in A. Dark areas correspond to regions where the orientation preference of adjacent pixels differs by at least 22.5° (corresponding to a rate of change of 1.7°/μm) to a maximum of 90° (6.8°/μm). **C:** Orientation preference map of ferret area 17, obtained in a manner similar to A. **D:** Map of orientation gradient obtained from C. For maps A and B, lateral is up and anterior is to the left. For maps C and D, anterior is up and medial is to the left. Scale bar = 1 mm.

particular orientation (including opposite directions of motion) by the image obtained for the blank stimulus. Composite maps of orientation magnitude and angle of orientation preference were obtained by computing the vector average of all the single-orientation maps pixel-by-pixel in the following way:

$$M = \sqrt{a^2 + b^2} \qquad \theta = \tan^{-1}(b/a)$$

$$a = \Sigma_i R_i \cos(2\theta_i),\ b = \Sigma_i R_i \sin(2\theta_i),$$

where M is orientation vector magnitude and θ is angle of preferred orientation. R_i is the signal strength and θ_i is the stimulus orientation corresponding to the ith map.

Orientation angle maps were displayed in color, with adjacent colors representing adjacent stimulus orientations. The vector angle (A) of the pixels was binned to the nearest stimulus angle.

Orientation gradient maps were computed from the orientation angle maps as the two-dimensional spatial derivative at each pixel:

$$\text{Spatial gradient} = \sqrt{dx^2 + dy^2}$$

$$dx = |\theta_{(x+1,y)} - \theta_{(x,y)}| \qquad \text{and} \qquad dy = |\theta_{(x,y+1)} - \theta_{(x,y)}|$$

where values of dx or dy greater than 90° were subtracted from 180°, such that the maximum difference in preferred angle was 90°.

Other calculations are described in Results.

RESULTS

Images of orientation domains

Data from nine cats and three ferrets were used for this study, based on 1) the high signal-to-noise ratio in the maps, and 2) response images obtained at eight stimulus orientations (16 directions). Single orientation maps of cortical responses to moving gratings in area 17 of cat (Fig. 1A,B) and ferret (Fig. 2A,B) show segregated regions or patches of activity, termed "orientation domains," that are spatially complementary for orthogonal stimulus orientations. Images with improved contrast for better visualization of orientation domains can be obtained by dividing such pairs of maps. Figure 1C, for cat, shows a map of 22.5° orientation domains divided by 112.5° domains; Figure 2C, for ferret, shows a map of 0° orientation domains divided by 90° domains. There is also a smooth change in the spatial location of orientation domains activated by intermediate stimulus orientations. Figures 1D and 2D show the vasculature of the imaged cortical region in cat and ferret, respectively. The high signal quality in the

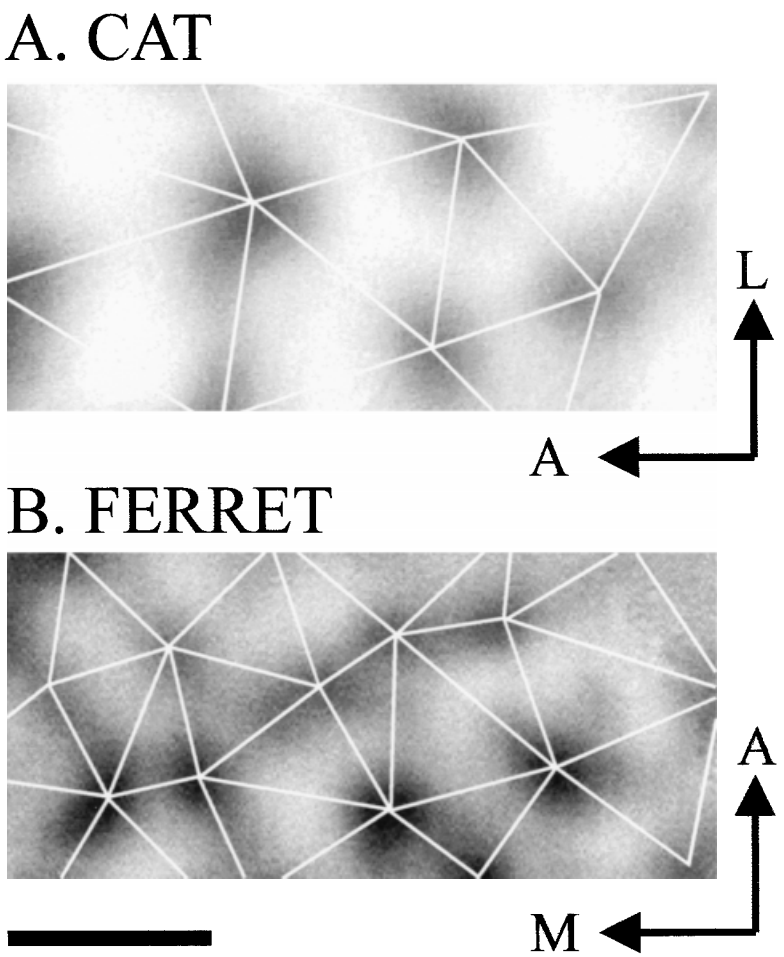

Fig. 4. Single-orientation maps from area 17 of (**A**) cat and (**B**) ferret, showing the lattice of iso-orientation domains. Scale bar = 1 mm.

unsmoothed single-orientation maps (Figs. 1A,B, 2A,B) is evident in the lack of significant blood vessel artifacts in these images. The mean density of iso-orientation domains is 1.49 ± 0.19/mm^2 in cat area 17 compared to 2.73 ± 0.35/mm^2 in ferret. These basic features of the cat and ferret maps are consistent across all imaged animals.

Maps of orientation preference

Orientation preference or angle maps in area 17, derived from single condition maps by vector averaging (see Materials and Methods), are shown in Figure 3A for cat and Figure 3C for ferret. The most obvious feature of these maps is the radial arrangement of orientation preference in a "pinwheel-like" manner (Bonhoeffer and Grinvald, 1993; Bonhoeffer et al., 1995) and the periodicity of these structures. We find a pinwheel density in cat of 2.4 ± 0.47/mm^2 (n = 9 animals) and in ferret of 5.5 ± 1.25/mm^2 (n = 3 animals). As expected for a continuous mapping of orientation, in which one orientation domain connects two pinwheels of opposite rotational sense, the pinwheel density is approximately twice the orientation domain density. Furthermore, the density of pinwheels found in ferret area 17 is roughly twice that found in cat area 17.

To examine whether the higher density of pinwheels in ferret compared to cat correlates with a difference in the regularity of mapping, we computed the two-dimensional spatial derivative of the orientation preference maps. Figure 3B,D show such orientation gradient maps for cat and ferret, respectively. White regions denote smooth changes in the orientation vector (with low orientation gradient), whereas discontinuous regions (with high orientation gradient), where the vector angle of adjacent pixels changes by at least 22.5° (1.7°/μm), are coded black. Regions of high orientation gradient, which include both pinwheel centers as well as "fracture zones" (discrete bands that extend between pinwheel centers), occupy 2.41% of the mapped region in cat area 17 compared to 4.25% in ferret area 17 (Fig. 3B,D). Thus, the ferret map is indeed less regular and more discontinuous than the cat map.

Spatial spread of activity

The spread of activity in a single orientation domain, in response to stimulation with gratings of a given orientation, reflects the net orientation tuning of neuronal populations in the imaged cortex: Broadly tuned neurons would

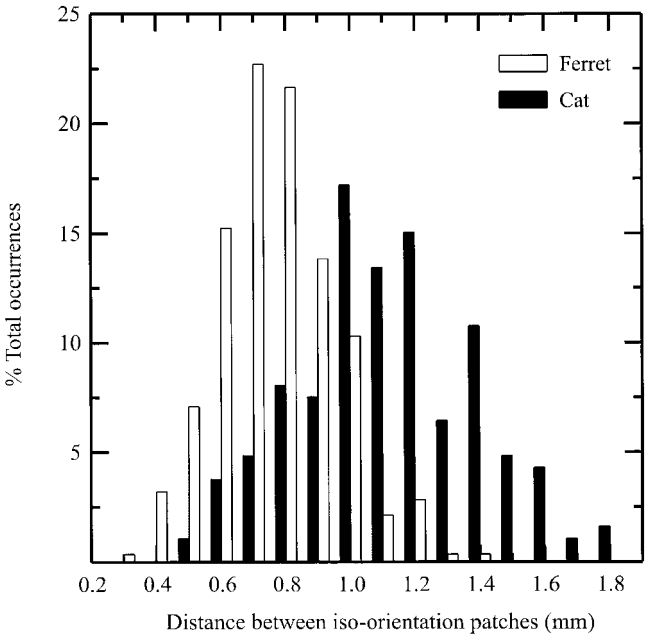

Fig. 5. Distribution of the spacing of iso-orientation domains in cat and ferret area 17. Distances between neighboring iso-orientation domains (as in Fig. 4) in each of the eight single-orientation maps for cat and ferret are binned to the nearest 0.1 mm.

lead to large orientation domains, and to greater overlap between orientation domains, whereas narrowly tuned neurons would have the opposite effect. Thus, an analysis of orientation domain size relative to spacing between domains provides a measure of the orientation tuning of neurons in cortex. Because orientation domains are spaced closer together in ferrets than in cats (Fig. 2, see also below), it is of interest to examine domain size in the two species. One possibility is that the ferret map has proportionately smaller orientation domains in keeping with smaller spacing between orientation domains; this would be reflected in similar tuning widths of imaged pixels in cat and ferret. An alternative possibility is that the map in ferret contains proportionately larger orientation domains, reflected in broader orientation tuning widths of its imaged pixels. Quantitative assessments of interdomain spacing, orientation domain size, and tuning widths of pixels in cat and ferret maps support the first possibility.

Iso-orientation domains imaged in response to a grating of any orientation form a quasi-regular lattice in both animals (Fig. 4). The distribution of the spacing between iso-orientation domains, measured for all well-defined domains from the 8 single-orientation maps in one animal each (Fig. 5), confirms that the domains are significantly more closely spaced in ferret area 17 (mean and SD, 0.72 ± 0.18 mm, $n = 282$) compared to cat (mean and SD, 1.07 ± 0.27 mm, $n = 186$; $P < .01$, Mann-Whitney U-test).

To evaluate the size of orientation domains relative to their spacing, and hence the relative spatial spread of activity, we compared domains that were spaced a known distance apart in the cat and ferret maps. We constructed line profiles of activity from the single-orientation maps, starting in each case at one domain center and ending at an adjacent domain center. Each line profile was obtained by normalizing the response of all pixels on the line joining two neighboring iso-orientation domains by the value at the starting location. Figure 6A shows an average of 29 such line profiles obtained for cat and 43 profiles for ferret. The two profiles are similar, with smooth variations in activity from a local maximum at the center of an orientation domain, to a local minimum at approximately the mid-point between domain centers, back to a local maximum at the next domain center. The half-width at half-height for the cat profile is 270 μm, indicating a mean domain width of 540 μm, which is almost exactly half of the center-to-center spacing between these very same domains. The half-width at half-height for the ferret profile is 185 μm, indicating a mean domain width of 370 μm, a value close to half of the spacing between these same domains. If the line profiles of activity for the cat and ferret maps are normalized to the mean inter-domain spacing in the two species, the profiles match closely (Fig. 6B). This indicates that the representations of single orientations in the cat and ferret maps are approximately scaled versions of each other.

The fact that the size of individual orientation domains relative to interdomain spacing is the same in cat and ferret suggests a similarity in orientation tuning widths imaged optically in the two species. Indeed, orientation tuning widths of pixels in the two maps are similar, when considered both across the entire map and in different ranges of orientation magnitude (described below).

Magnitude of orientation vector

The magnitude of orientation preference obtained by vector averaging the response of a pixel to the eight stimulus orientations (Materials and Methods) is a measure of both the tuning of responses for orientation and the depth of response modulation between optimal and orthogonal orientations. The frequency histogram of normalized orientation magnitudes in the two species is shown in Figure 7. Orientation magnitudes in cat are significantly greater than those in ferret ($P < .01$, t-test); the mean orientation magnitude in cat (0.42 ± 0.18) is nearly twice that in ferret (0.22 ± 0.11).

We analyzed the spatial variation of orientation magnitude and gradient over the entire map to examine the relationship between the two. Figure 8A and D show maps of orientation magnitude in cat and ferret; Figure 8B and E show the magnitudes color-coded to depict various percentile ranges (i.e., contours of orientation magnitude). Figure 8C and F show for comparison the fracture maps of cat and ferret (where changes in orientation preference of adjacent pixels by 67.5°, or 5.1°/μm, and greater are shown in black). Clearly, the regions of lowest orientation magnitude are coextensive with pinwheel centers and fractures. In addition, the high-magnitude regions include broad swaths of cortex where orientation remains constant or varies smoothly over a limited range (see Fig. 3).

Orientation tuning width

We next examined the relationship between orientation magnitude and tuning width in the cat and ferret maps. One hypothesis with respect to zones of low orientation magnitude (fracture zones and pinwheel centers) is that cells in these regions have broader tuning width than other regions of the map. An alternative hypothesis is that cells in fracture zones need not be tuned more broadly for orientation compared to regions where orientation is constant or changes smoothly; rather, cells close together in

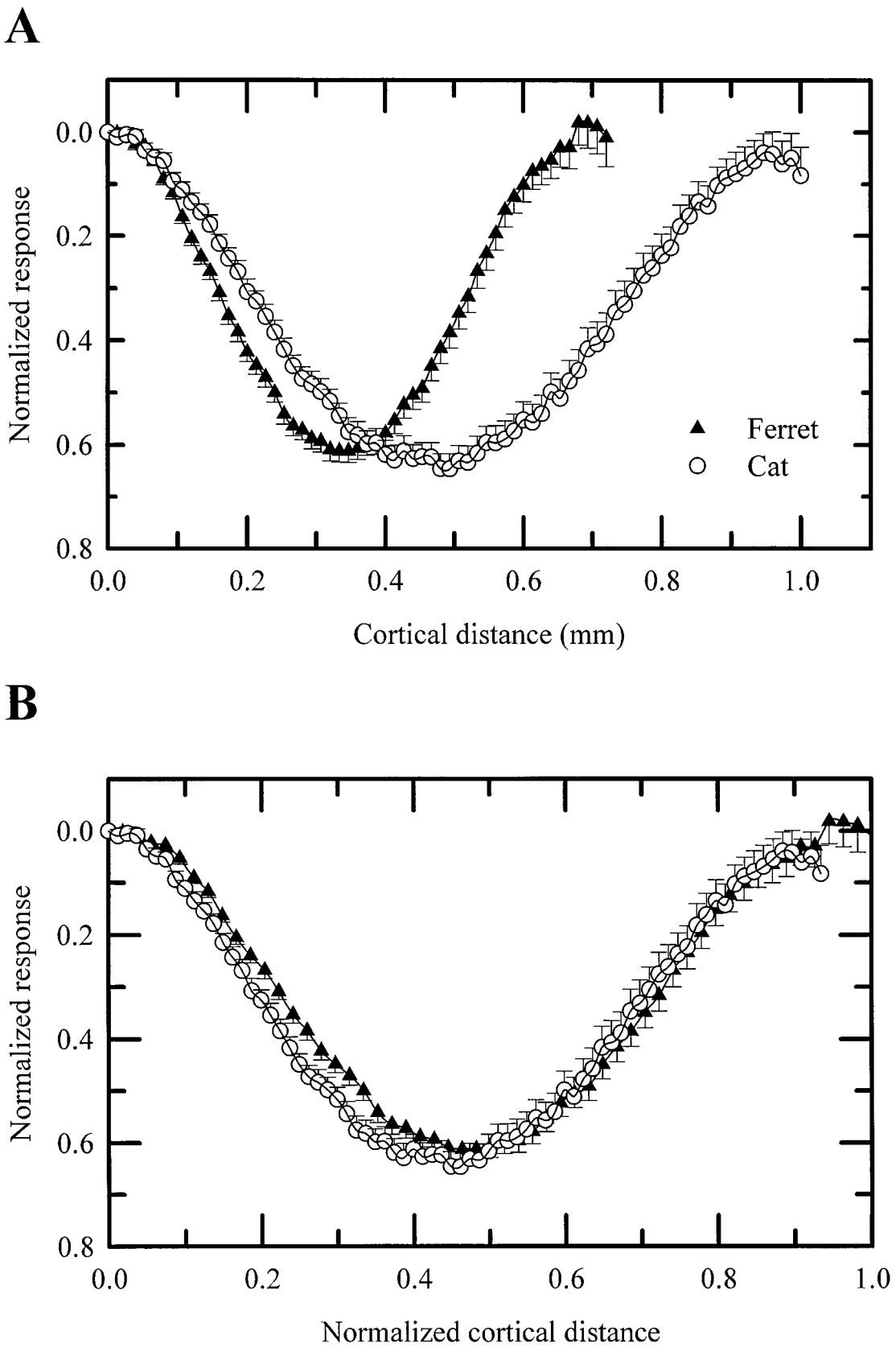

Fig. 6. **A:** Mean profile of response amplitude vs. distance, showing the spatial spread of activity from the center of a domain in the cat and ferret single-orientation maps. Each line profile is the normalized response (see text) of all pixels on the line joining centers of two neighboring iso-orientation domains with a mean interdomain distance between 0.9 mm and 1.1 mm for cat and between 0.6 mm and 0.8 mm for ferret. Note that 0 represents maximal activity and 1 represents activity similar to the background. **B:** Same data as in A, but the absolute cortical distance is now normalized to the mean interdomain distance for cat and ferret obtained from Figure 5. Bars denote standard error.

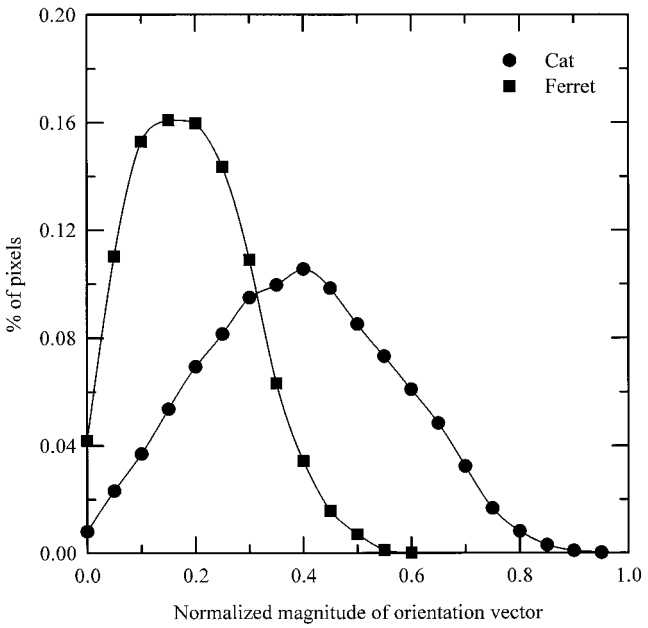

Fig. 7. Histogram showing the distribution of normalized orientation magnitude across the entire map for cat and ferret. Normalized vector magnitude values are binned to the nearest 0.05. The mean magnitudes for cat (0.42 ± 0.18) and ferret (0.22 ± 0.11) represent absolute vector magnitudes of 31.4×10^{-4} (SD: 1.33×10^{-4}) and 16.4×10^{-4} (SD: 0.82×10^{-4}), respectively.

these regions would have wide variations in preferred orientations. An analysis of tuning width as a function of orientation magnitude across the map generally supports the latter hypothesis.

To compute orientation tuning curves for individual pixels, the response of each pixel to different stimulus orientations was obtained from the eight single-orientation maps. These values were then normalized, such that 0 represented maximal activity and 1 represented activity similar to background (with the animal viewing a blank stimulus), and plotted relative to the vector angle binned to the nearest stimulus angle. It is important to note that these tuning curves represent the mean tuning of neurons under pixels each summing activity over a region approximately 13 μm × 13 μm. Figure 9 shows mean optical tuning curves over the entire map for cat and ferret, for different orientation magnitudes ranging from the lowest values (0–5 percentile) to the highest (90–100 percentile). Pixels in both cat (Fig. 9A) and ferret (Fig. 9B) have similar mean tuning widths (defined as the width at half-height); indeed, the mean width of orientation tuning across all pixels (mean ± SD for cat 71.4° ± 4.7°; for ferret 76.5° ± 4.5°) remains nearly the same, whereas the amplitude of modulation between maximal and minimal response varies approximately fourfold in cat and approximately fivefold in ferret. Importantly, even the pixels with the lowest 5% of orientation magnitude, which are essentially co-extensive with pinwheel centers and associated fractures (Fig. 8), have an average tuning width (cat: 78.3°, ferret: 81.2°) that is only slightly broader than that of pixels in the 90–100% magnitude range (cat: 68.5°, ferret: 70.4°), which are near the centers of iso-orientation domains. We note again that these tuning widths represent the means of many pixels, with tuning measured optically. The tuning of individual pixels can show variability that increases as orientation magnitude decreases. Importantly, the similarity in orientation tuning widths in the cat and ferret maps is consistent with the proportional representation of orientation domain size and spacing in the two species.

Pinwheel centers and fracture lines

Although the representation of single orientations in cat appears to be an expanded version of that in ferret, it is also evident that a greater proportion of the map has discontinuities or fractures in ferret compared to cat (Fig. 3). One reason is the lower overall magnitude of orientation preference in ferret (Fig. 7). If fractures are associated with a certain absolute level (or lower) of orientation magnitude, it follows that a greater portion of the ferret map would be devoted to fractures. For example, a normalized magnitude of 0.05 or lower would comprise about 1% of pixels in cat (0.89%) but roughly 2% in ferret (1.80%) (Fig. 7). Not only do fractures occupy a greater portion of the ferret map, the fractures have a consistent relationship to pinwheel centers: Fractures extend through pinwheel centers, and fracture lines often link adjacent pinwheel centers. Pinwheel centers represent regions where domains of activity elicited by different stimulus orientations overlap (Bonhoeffer et al., 1995). We examined whether the overlap between orientation domains in ferrets is greater than in cats and extends between pinwheel centers to include fracture lines.

Figure 10 shows the spatial relationship between pixel orientation in the vector angle map and the underlying map of orientation gradient. Starting with a pixel in the center of an orientation domain, we derived from the orientation angle map the region over which the angle difference between the central pixel and any other pixel was ±22.5°. The contours are shown in Figure 10A,B for cat, and Figure 10C,D for ferret, overlying the map of orientation preference and orientation gradient, respectively. These figures demonstrate two features of orientation packing. First, the core zone within an orientation domain of a single-orientation map is generally coextensive with the representation of that orientation (correct to a narrow range of angle) in the vector angle map. This is what we would otherwise intuit, for high signal strength at one orientation at any pixel would contribute significantly to the orientation vector at that pixel. Second, at their edges the orientation domains encroach into the representations of other orientations in the vector angle map; however, the extent of encroachment is greater in ferret than in cat and is preferentially aligned along the line linking pinwheel centers (Fig. 10C). These extended regions of overlap between domains of different orientations represent fracture lines in the gradient map in ferret (Fig. 10D); the gradient map in cat typically does not show a similar fracture line (Fig. 10B).

DISCUSSION

Maps of orientation preference in primary visual cortex of cats and ferrets, revealed by optical imaging of intrinsic signals, are similar in some respects but different in others. Maps in both species contain a quasi-periodic distribution of iso-orientation domains which are organized into a lattice of pinwheels. However, the spatial density of iso-orientation domains and pinwheels in ferret

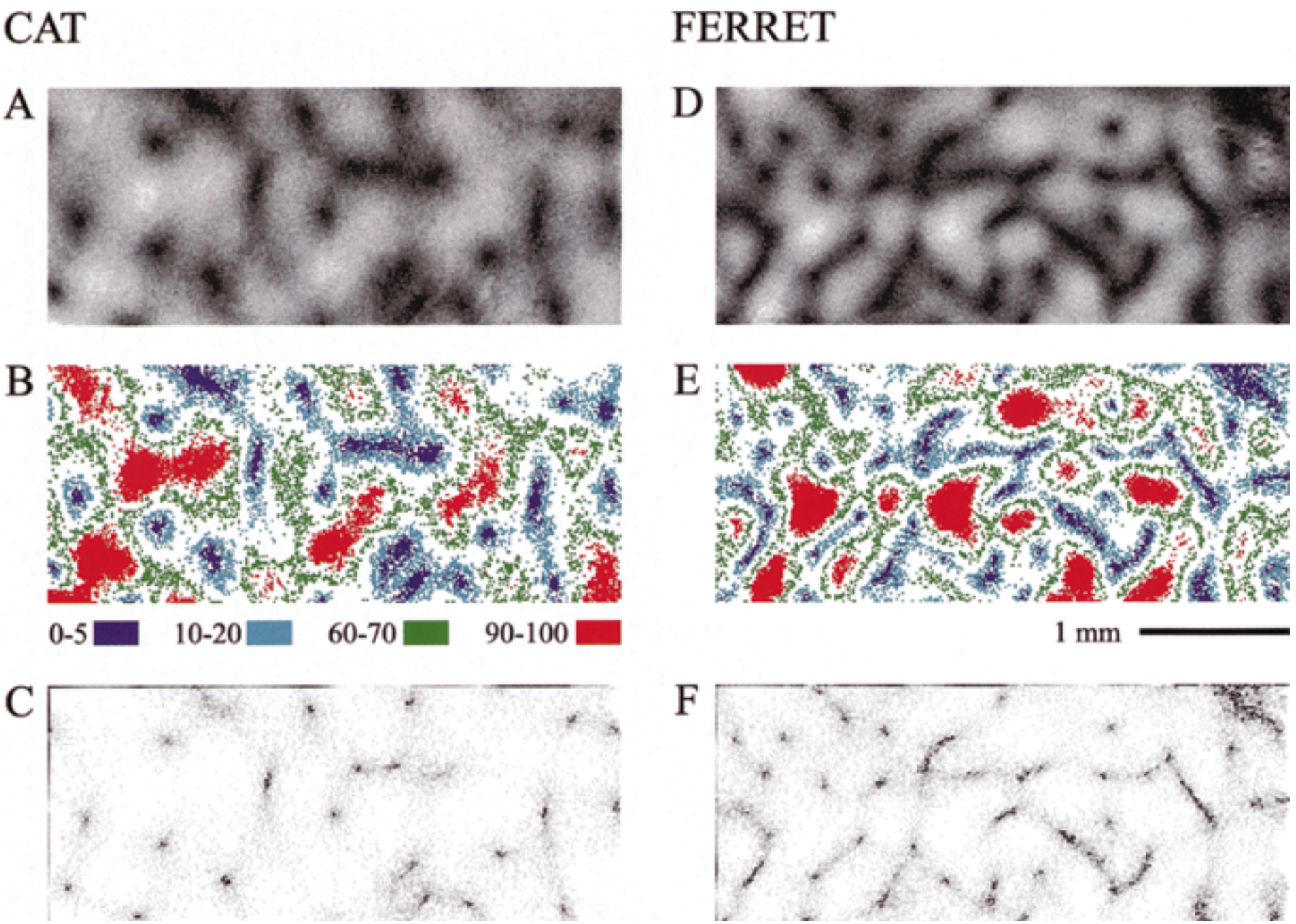

Fig. 8. Maps of orientation vector magnitude and orientation gradient for (**A–C**) cat and (**D–F**) ferret area 17. A,D: Maps of vector magnitude, with increasing magnitudes coded from black to white. B,E: Color-coded maps showing regions of different percentile ranges of normalized vector magnitude. C,F: Orientation gradient maps, in which adjacent pixels differing in orientation preference by 67.5° (5.1°/μm) or more are coded black.

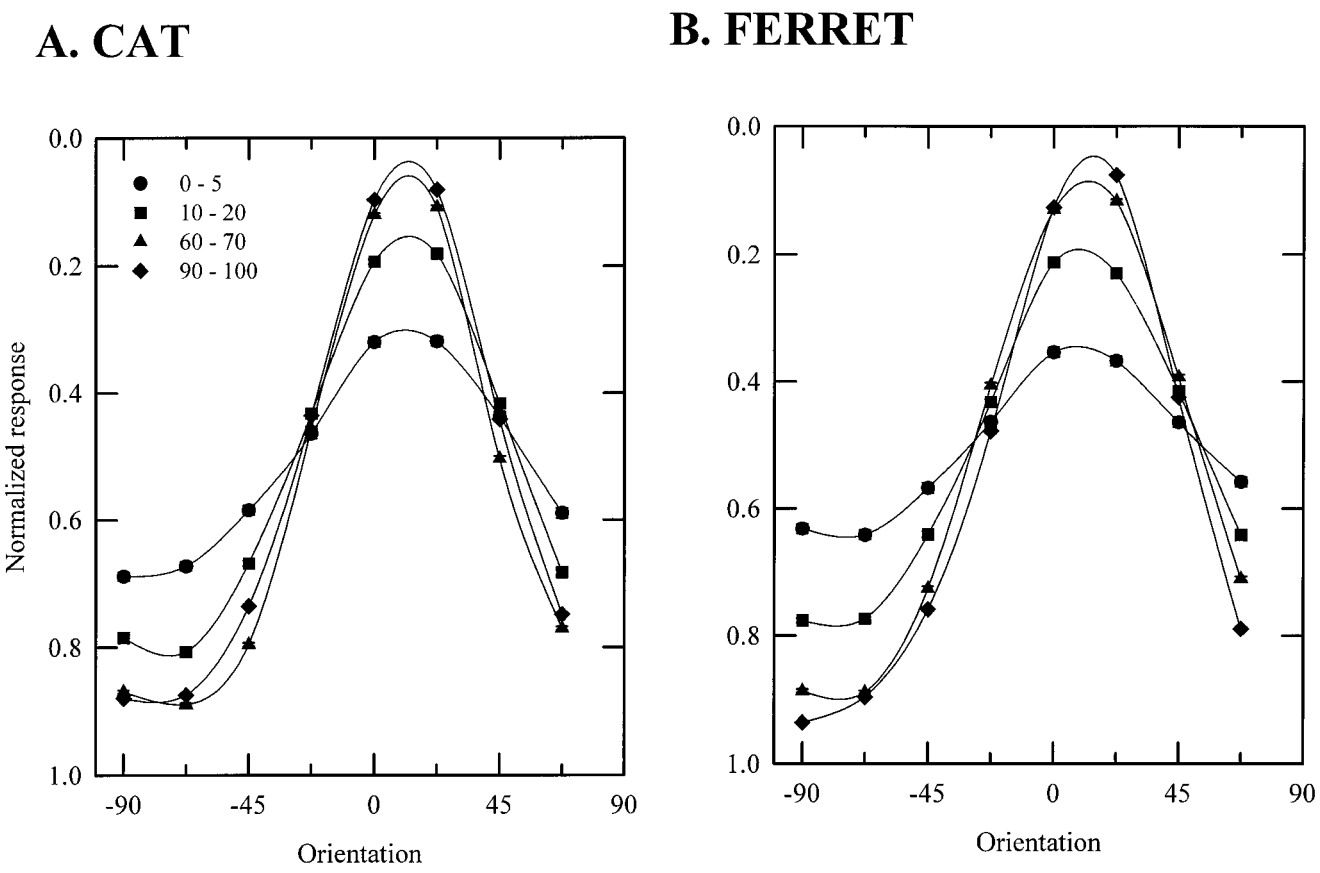

Fig. 9. Mean optical tuning curves of pixels in (**A**) cat and (**B**) ferret maps, in different percentile ranges of orientation vector magnitude (compare with Fig. 8, and see text for details).

is nearly twice that in cat. Furthermore, the ferret map contains more discontinuities, or fractures, where orientation changes abruptly across adjacent pixels. While spacing between adjacent iso-orientation domains is less in ferret compared to cat, the size of each domain is proportionately less in ferret as well. Consistent with this finding, orientation tuning width of individual pixels is similar in the two maps. A major difference between the two maps is the magnitude of orientation preference (magnitude of the orientation vector): These are much lower in ferret compared to cat. Contours of lowest orientation magnitude are co-extensive with pinwheel centers and fracture lines. However, these loci do not represent regions with broad orientation tuning of pixels; rather, the width of orientation tuning appears to be generally similar across the map. The greater incidence of fractures in the ferret map is due to lower overall orientation magnitude compared to cat and to proportionately greater overlap between domains of different orientations along fracture lines linking pinwheel centers.

Comparison with other studies of cat and ferret area 17

Our data on the overall organization of orientation maps compares well with previous work in cat and ferret area 17 using either optical imaging or 2-deoxyglucose (2-DG) labeling of orientation domains. The one previous study (Bonhoeffer et al., 1995) in which cat area 17 was imaged and the maps were analyzed in some detail found a pinwheel density of 2.1 pinwheel-centers/mm^2, a value similar to 2.4 pinwheel-centers/mm^2 found by us. Bonhoeffer et al. (1995) also noted that pinwheel centers had low magnitude of the orientation vector, whereas orientation magnitude was highest in the middle of iso-orientation patches. Optical maps of orientation selectivity in ferret area 17 have not been previously analyzed in any detail, although the maps shown by Weliky et al. (1995, 1996) resemble our maps at least qualitatively in terms of pinwheel density and size and disposition of iso-orientation domains.

Our optically imaged single-orientation maps in cat and ferret area 17 are broadly similar to iso-orientation patterns obtained with 2-DG autoradiography. The imaged maps show a patchy pattern of iso-orientation zones, as distinct from a pattern of iso-orientation bands or "beads" labeled with 2-DG (Schoppman and Stryker, 1981; Löwel and Singer, 1987). Although there are several possible reasons for a spread of label in 2-DG experiments, the average spacing of 1.08 mm between orientation domains in cat area 17 suggested by Albus and Sieber (1984) using 2-DG is similar to the spacing of 1.07 mm obtained by us using optical imaging. In ferret area 17, using 2-DG, Redies et al. (1990) found the periodicity of iso-orientation domains to be 1.4 cyc/mm, corresponding to a mean spacing of 0.7 mm, whereas we found a mean spacing of 0.72 mm when using optical imaging.

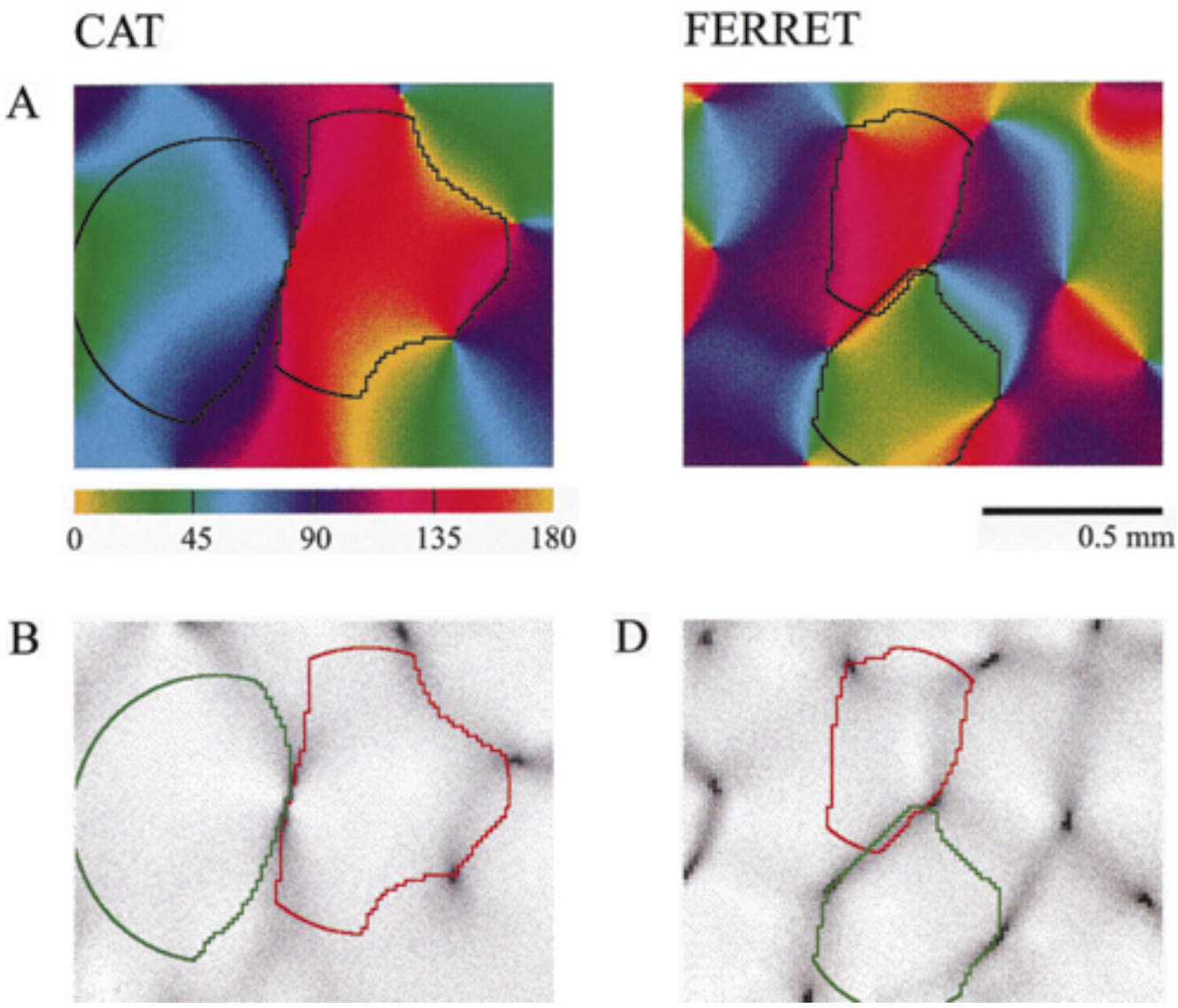

Fig. 10. Size of orientation domains for (**A,B**) cat and (**C,D**) ferret. Contours enclose areas in which the change in vector angle of a pixel is within ± 22.5° of the central pixel. Underlying maps are of orientation angle (top) and orientation gradient (bottom).

Orientation tuning in cat and ferret area 17

Our optical maps indicate that 1) orientation magnitude is lower, on average, in ferret area 17 compared to cat, and 2) the width of orientation tuning measured optically for single pixels is similar for cat and ferret.

The magnitude of the orientation vector, as calculated by us for single pixels, is equivalent to measuring the amplitude of the second harmonic component along stimulus direction (Wörgotter and Eysel, 1987) and represents a combined measure of orientation tuning width and orientation-dependent response modulation. An equivalent measure for single neuron responses has been termed the orientation selectivity index (Chapman and Stryker, 1993) and is calculated from the second harmonic component of single neuron responses (normalized by the sum of the dc component and second harmonic). Their measure is consistently higher in cat than in ferret. The median index in cat is about 20% larger than that in ferret, and the peak index (i.e., the most sharply tuned cells) is also larger in cat by a similar amount. These data are consistent with our optical measurements of orientation magnitude.

The orientation tuning width of single neurons, defined as the width at half-maximal response, is narrower in cat area 17 (see Orban, 1984, for review) compared to ferret (Roe et al., 1992). Orientation tuning widths of single pixels obtained by optical recording in cat are much broader than average tuning widths of simple cells in cat area 17 obtained by single unit recording (mean values from several studies, 28°–44°; see Orban, 1984), but only slightly broader than tuning widths of complex cells (mean 38°–63°; op. cit.). The tuning widths of single pixels in ferret area 17 are actually comparable to average single

unit widths (ca. 72° at $1/\sqrt{2}$ height, Roe et al., 1992; simple and complex cells were not studied separately). In general, the optically imaged tuning widths may be larger for the following reasons: 1) unlike single unit spikes, optical signals are metabolic signals arising not only from spiking activity but also from subthreshold activity (Das and Gilbert, 1995; Toth et al., 1996), 2) each pixel in the optical images encompasses an area of 13 μm × 13 μm, so that the signal represents an average of several neurons, 3) the source of the signal, although obtained from the superficial cortical layers, might include a larger volume of tissue. All of these factors contribute to spatial smearing of optically imaged compared to single unit activity.

The fact that pixels near pinwheel centers have orientation tuning widths that are only slightly broader than those in iso-orientation regions is consistent with a recent brief report of single neuron tuning widths at identified locations within an orientation map in cat area 17 (Gödecke et al., 1996; but see Ruthazer et al., 1996).

Anatomical correlates of orientation domain size and spacing

Our data demonstrate that the size of individual iso-orientation domains and their spacing are closely related in the orientation maps. There is good evidence that the spacing between iso-orientation domains reflects clustered long-range intracortical projections within the superficial layers of visual cortex. In area 17, horizontal connections link cells with similar orientation preference, as demonstrated by combining tracer injections in cortex with 2-DG labeling in cats (Gilbert and Wiesel, 1989; Löwel and Singer, 1992) or by combining tracers with optical imaging in tree shrews (Bosking et al., 1997). The mean spacing between iso-orientation domains imaged optically in cat (1.07 mm) correlates well with the mean spacing between patches of label following focal injections of tracers (Luhmann et al., 1989: 1.05 mm; Callaway and Katz, 1990: ca. 1 mm; Kisvarday and Eysel, 1992: 1.1 mm; Lubke and Albus, 1992: 1 mm; Galuske and Singer, 1996: 0.82 mm). In ferret area 17, combined tracer injection and optical imaging demonstrate that horizontal connections are patchy and target iso-orientation domains (Sharma et al., 1995), with the mean interpatch distance (0.7 mm) resembling the mean spacing between iso-orientation domains (0.72 mm). Similarly, focal injections in ferret area 17 reveal a center-to-center spacing of 0.6–0.7 mm in the horizontal spread of label (Rockland, 1985). Interestingly, unlike area 17 of cat and ferret where horizontal connections link adjacent iso-orientation domains, horizontal connections in monkey area 17 appear to link only iso-orientation domains related to the same eye, skipping intervening domains related to the other eye (Malach et al., 1993).

Thalamocortical afferents provide the initial drive for orientation tuning in cortex (Hubel and Wiesel, 1962). We hypothesize that the size of iso-orientation domains is related to the spread of thalamocortical arbors. Iso-orientation domains in cat area 17 (mean diameter, 0.54 mm) are comparable to the sizes of single geniculocortical X axon arbors (mean arbor diameter, ca. 0.5 mm) or individual clumps of Y axon arbors within area 17 (Humphrey et al., 1985a). Iso-orientation domains in ferret area 17 are smaller (mean diameter, 0.37 mm). Although single LGN axon arbors in ferret area 17 have not been examined to date, ocular dominance columns in ferrets revealed by intraocular injections of anterogradely transported tracers show these columns to be 0.3–0.7 mm in width (Law et al., 1988). The columns, particularly at the lower end of sizes, are smaller than similarly labeled columns in cats, which are 0.5–1.0 mm in width (LeVay et al., 1978). It is reasonable to expect from such population labeling (e.g., Ferster and LeVay, 1978) that single X axon arbors in ferrets would be proportionately smaller than those in cats, and comparable to sizes of iso-orientation domains.

An argument for relating orientation domain sizes to thalamocortical arbors can be made by comparing the two across other species and cortical areas in which they have been defined. The smallest optically imaged orientation domains are seen in area 17 of tree shrews (Pucak et al., 1996: mean diameter, 0.25 mm) and macaque monkeys (Blasdel, 1992; Malach et al., 1993: mean diameter 0.25–0.3 mm). The most compact thalamocortical axons in area 17 have mean arbor widths of ca. 0.25 mm in both tree shrews (Raczkowski and Fitzpatrick, 1990) and macaque monkeys (Blasdel and Lund, 1983). The next larger orientation domains, and thalamocortical arbors, are seen in ferret and cat area 17, respectively (described above). The largest orientation domains have been imaged in cat area 18 (Bonhoeffer and Grinvald, 1993: mean diameter, ca. 1.0 mm). Axons of LGN Y cells innervate area 18 in cats and have more extensive terminations than in area 17; the arbor widths are typically 1 mm or more (Humphrey et al., 1985b).

In each of these species and areas, the relationship between orientation domain size and interdomain distance appears to hold: Interdomain distances are smallest, and hence the density of pinwheel centers are highest, in macaque area 17, intermediate in ferret and cat area 17, and lowest in cat area 18. Thus, we propose that the extent of the smallest thalamocortical projections bears a close and systematic relationship to the spacing between intracortical horizontal projections in visual cortex. This would appear to be an anatomical substrate for the map of orientation specificity in visual cortex and a hypothesis that can be examined in future experiments.

ACKNOWLEDGMENTS

We thank Bhavin Sheth for his help in initial experiments and Dae-Shik Kim for helpful discussions. S.C.R. was supported by a postdoctoral fellowship from the Markey Foundation. This study was supported by NIH grant EY07023 to M.S.

LITERATURE CITED

Albus, K., and B. Sieber (1984) On the spatial arrangement of iso-orientation bands in cat's visual cortical areas 17 and 18: a ^{14}C-deoxyglucose study. Exp. Brain Res. *56*:384–388.

Blasdel, G.G. (1992) Orientation selectivity, preference, and continuity in monkey striate cortex. J. Neurosci. *12*:3139–3161.

Blasdel, G.G., and J. Lund (1983) Termination of afferent axons in macaque striate cortex. J. Neurosci. *7*:1389–1413.

Bonhoeffer, T., and A. Grinvald (1993) The layout of iso-orientation domains in area 18 of cat visual cortex. Optical imaging reveals pinwheel-like organization. J. Neurosci. *13*:4157–4180.

Bonhoeffer, T., D.-S. Kim, D. Malonek, D. Shoham, and A. Grinvald (1995) Optical imaging of the layout of functional domains in area 17 and across the area 17/18 border in cat visual cortex. Eur. J. Neurosci. *7*:1973–1988.

Bosking, W.H., Y. Zhang, B. Schofield, and D. Fitzpatrick (1997) Orientation selectivity and the arrangement of horizontal connections in the tree shrew striate cortex. J. Neurosci. *17*:2112–2127.

Callaway, E.M., and L.C. Katz (1990) Emergence and refinement of clustered horizontal connections in cat striate cortex. J. Neurosci. *10:*1134–1153.

Chapman, B., and M.P. Stryker (1993) Development of orientation selectivity in ferret visual cortex and effects of deprivation. J. Neurosci. *13*:5251–5262.

Das, A., and C.D. Gilbert (1995) Long-range horizontal connections and their role in cortical organization revealed by optical recording of cat primary visual cortex. Nature *375:*780–784.

Ferster, D., and S. LeVay (1978) The axonal arborizations of lateral geniculate neurons in the striate cortex of the cat. J. Comp. Neurol. *182:*923–944.

Galuske, R.A.W., and W. Singer (1996) The origin and topography of long-range intrinsic projections in cat visual cortex: a developmental study. Cereb. Cortex *6:*417–430.

Gilbert, C.D., and T.N. Wiesel (1989) Columnar specificity of intrinsic horizontal and corticocortical connections in cat visual cortex. J. Neurosci. *9:*2432–2442.

Gödecke, I., P.E. Maldonado, C.M. Gray, and T. Bonhoeffer (1996) Response properties of neurons in and near pinwheel centers in orientation preference maps of cat visual cortex. Soc. Neurosci. Abstr. *22:*641.

Hubel, D.H., and T.N. Wiesel (1962) Receptive fields, binocular interaction and functional architecture in the cats visual cortex. J. Physiol. (Lond.) *160:*106–154.

Hubel, D.H., and T.N. Wiesel (1974) Uniformity of monkey striate cortex: a parallel relationship between field size, scatter and magnification factor. J. Comp. Neurol. *158:*295–302.

Humphrey, A.L., M. Sur., D.J. Uhlrich, and S.M. Sherman (1985a) Projection patterns of individual X- and Y-cell axons from the lateral geniculate nucleus to cortical area 17 in the cat. J. Comp. Neurol. *233:*159–189.

Humphrey, A.L., M. Sur, D.J. Uhlrich, and S.M. Sherman (1985b) Termination patterns of individual X- and Y-cell axons in the visual cortex of the cat: projections to area 18, to the 17/18 border region, and to both areas 17 and 18. J. Comp. Neurol. *233:*190–212.

Kaas, J.H. (1988) Development of cortical sensory maps. In P. Rakic and W. Singer (eds): Neurobiology of Neocortex. New York: Wiley, pp. 101–113.

Kim, D.-S., and T. Bonhoeffer (1994) Reverse occlusion leads to a precise restoration of orientation preference maps in visual cortex. Nature *370:*370–372.

Kisvarday, Z.F., and U.T. Eysel (1992) Cellular organization of reciprocal patchy networks in layer III of cat visual cortex (area 17). Neuroscience *46:*275–286.

Law, M.I., K.R. Zahs, and M.P. Stryker (1988) Organization of primary visual cortex (area 17) in the ferret. J. Comp. Neurol. *278:*157–180.

LeVay, S., M.P. Stryker, and C.J. Shatz (1978) Ocular dominance columns and their development in layer IV of cat's visual cortex: a quantitative study. J. Comp. Neurol. *179:*223–244.

Löwel, S., and W. Singer (1987) Topographic organization of the orientation column system in large flat-mounts of cat visual cortex. J. Comp. Neurol. *255:*401–415.

Löwel, S., and W. Singer (1992) Selection of intrinsic horizontal connections in the visual cortex by correlated neuronal activity. Science *255:*209–212.

Lubke, J., and K. Albus (1992) Rapid rearrangement of intrinsic tangential connections in the striate cortex of normal and dark reared kittens: lack of exuberance beyond the second postnatal week. J. Comp. Neurol. *323:*42–58.

Luhmann, H.J., W. Singer, and L. Martinez-Millan (1989) Horizontal interactions in cat striate cortex: I. anatomical substrate and postnatal development. Eur. J. Neurosci. *2:*344–357.

Malach, R., Y. Amir, M. Harel, and A. Grinvald (1993) Relationship between intrinsic connections and functional architecture revealed by optical imaging and *in vivo* targeted biocytin injections in primate striate cortex. Proc. Natl. Acad. Sci. U.S.A. *90:*10469–10473.

Merzenich, M.M., J.H. Kaas, J. Wall, R.J. Nelson, M. Sur, and D. Felleman (1983) Topographic reorganization of somatosensory cortical areas 3B and 1 in adult monkeys following restricted deafferentation. Neuroscience *8:*33–55.

Orban, G.A. (1984) Neuronal Operations in the Visual Cortex. Berlin: Springer.

Pucak, M.L., W.H. Bosking, and D. Fitzpatrick (1996) Optical imaging of tree shrew areas V1 and V2: maps of orientation preference and rules of interconnectivity. Soc. Neurosci. Abstr. *22:*1610.

Raczkowski, D., and D. Fitzpatrick (1990) Terminal arbors of individual, physiologically identified geniculocortical axons in tree shrew's striate cortex. J. Comp. Neurol. *302:*500–514.

Ratzlaff, E.H., and A. Grinvald (1991) A tandem-lens epifluorescence macroscope: hundred-fold brightness advantage for wide-field imaging. J. Neurosci. Methods *36:*127–137.

Redies, C., M. Diksic, and H. Riml (1990) Functional organization in the ferret visual cortex: a double-label 2-deoxyglucose study. J. Neurosci. *10:*2791–2803.

Rockland, K.S. (1985) Anatomical organization of primary visual cortex (area 17) in the ferret. J. Comp. Neurol. *241:*225–236.

Roe, A.W., S.L. Pallas, Y.H. Kwon, and M. Sur (1992) Visual projections routed to the auditory pathway in ferrets: receptive fields of visual neurons in primary auditory cortex. J. Neurosci. *12:*3651–3664.

Ruthazer, E.S., M.C. Crair, D.C. Gillespie, and M.P. Stryker (1996) Orientation tuning of single cells at pinwheel orientation singularities in kitten visual cortex. Soc. Neurosci. Abstr. *22:*277.

Schoppman, A. and M.P. Stryker (1981) Physiological evidence that 2-deoxyglucose method reveals orientation columns in cat visual cortex. Nature *293:*574–576.

Sharma, J., A. Angelucci, S.C. Rao, and M. Sur (1995) Relationship of intrinsic connections to orientation maps in ferret primary visual cortex: iso-orientation domains and singularities. Soc. Neurosci. Abstr. *21:*392.

Sur, M., M.M. Merzenich, and J.H. Kaas (1980) Magnification, receptive-field area, and "hypercolumn" size in areas 3b and 1 of somatosensory cortex in owl monkeys. J. Neurophysiol *44:*295–311.

Toth, L.J., S.C. Rao, D.-S. Kim, D. Somers, and M. Sur (1996) Subthreshold facilitation and suppression in primary visual cortex revealed by intrinsic signal imaging. Proc. Natl. Acad. Sci. U.S.A. *93:*9869–9874.

Weliky, M., K. Kandler, D. Fitzpatrick, and L.C. Katz (1995) Patterens of excitation and inhibition evoked by horizontal connections in visual cortex share a common relationship to orientation columns. Neuron *15:*541–552.

Weliky, M., W.H. Bosking, and D. Fitzpatrick (1996) A systematic map of direction preference in primary visual cortex. Nature *379:*725–728.

Wörgotter, F., and U.T. Eysel (1987) Quantitative determination of orientational and directional components in the response of visual cortical cells to moving stimuli. Biol. Cybern. *57:*349–355.